

# An Adaptable Route to Fast Coherent State Transport via Bang-Bang-Bang Protocols

Ya-Tang Yu,<sup>1,\*</sup> Hsin-Lien Lee,<sup>2,1</sup> Shao-Hung Chung,<sup>1</sup> Ting Hsu,<sup>2</sup>  
Guin-Dar Lin,<sup>2,3,4,5</sup> Yin-Cheng Chen,<sup>1</sup> and H. H. Jen<sup>1,5,†</sup>

<sup>1</sup>Institute of Atomic and Molecular Sciences, Academia Sinica, Taipei 10617, Taiwan

<sup>2</sup>Department of Physics and Center for Theoretical Physics,  
National Taiwan University, Taipei 10617, Taiwan

<sup>3</sup>Center for Quantum Science and Engineering, National Taiwan University, Taipei 10617, Taiwan

<sup>4</sup>Trapped-Ion Quantum Computing Laboratory, Hon Hai Research Institute, Taipei 11492, Taiwan

<sup>5</sup>Physics Division, National Center for Theoretical Sciences, Taipei 10617, Taiwan

(Dated: November 26, 2025)

Fast coherent state transport is essential to quantum computation and quantum information processing. While an adiabatic transport of atomic qubits guarantees a high fidelity of the state preparation, it requires a long timescale that defies efficient quantum operations. Here, we propose an adaptable and fast bang-bang-bang (BBB) protocol, utilizing a combination of forward- and backward-moving trap potentials, to expedite the coherent state transport. This protocol approaches the quantum speed limit under a harmonic trap potential, surpassing the performance by the forward-moving-only potential protocols. We further showcase the advantage of applying squeezed coherent state evolution under a deeper potential followed by a weaker one, where a design of symmetric squeezing potential transports promotes an even shorter timescale for genuine state preparation. Our protocols outperform conventional forward-moving-only methods, providing new insights and opportunities for rapid state transport and preparation, ultimately advancing the capabilities of quantum control and quantum operations.

**Introduction**—Fast coherent control of quantum states is crucial for state manipulation and preparation, which is essential in applications of quantum computation and quantum information [1–15]. To maintain the coherence of quantum states [16–21], an adiabatic transport is sufficient to fulfill this goal, but it takes a time longer than needed for efficient operations in practical quantum platforms. Getting around of this obstacle, a recipe of shortcuts to adiabaticity [21–25] provides fast routes to the coherent transport. This enables a rapid manipulation of quantum states—such as transporting a trapped particle—far faster than conventional adiabatic processes while still achieving the same high-fidelity final state.

A substantial body of works has focused on similar non-adiabatic protocols for transferring a motional ground state with high fidelity at the destination [26–31], since this state minimizes thermal effects on internal-state operations [32–35]. This is even more important for trapped-ion systems to suppress errors in gate operations [2, 36]. One commonly proposed optimal harmonic-trap trajectory, so-called ‘bang-bang’ (BB) control involving two instantaneous potential shifts [27, 29, 37–39], has shown an ultimate speed limit of transport using trapped-ion harmonic oscillators [40]. These instantaneous potential shifts are performed by an electrically controlled potential switch with a switching time far below the system’s responding time [41]. This demonstrates the capability of controlling a coherent state by sudden potential displacements and offers a faster route to transport a particle with high fidelity in a timescale of  $\pi/\omega_0$  [41], determined by the trap frequency  $\omega_0$ .

In this Letter, we propose an adaptable and fast bang-bang-bang (BBB) protocol, which facilitates the coherent

state transport and shortens the timescale, surpassing the timescale limited by the BB protocol. In contrast to the forward-moving-only potential protocol, we demonstrate that a backward movement of the potential—counterintuitive to the transport direction—is necessary to further reduce the transport time in harmonic potentials. By designing a combination of forward- and backward-moving trap potentials in the BBB protocol, we showcase that this protocol can reach the quantum speed limit as long as an instantaneous potential shift is sufficed under a harmonic trap potential. For practical consideration when the spatial confinement of a trap is limited, we adopt a squeezed coherent state evolution [42] projected on a deeper trap and manifest its advantage to further speed up the genuine state transport. Notably, the key for extra improvement on the timescale lies at a weaker trap frequency in the double-squeezed BBB (DS-BBB) protocol to further reduce the timescale for final state preparation. Our protocols outperform the conventional forward-moving-only potential methods, which offer unprecedented opportunities to fast state preparation and can be broadly implemented in both trapped-ion and neutral atom platforms.

**Model and phase-space dynamics**—We consider the transport of the motional state of a particle with mass  $m$  in a one-dimensional harmonic trap. Initially ( $t < 0$ ), the particle is in the ground state  $|0_{\text{init}}\rangle$  of the potential  $V_{\text{init}} = m\omega_0^2\hat{x}^2/2$ , where  $\hat{x}$  is the position operator. The goal is to transport the particle a distance  $d$  such that for  $t > T$ , it rests in the ground state  $|0_{\text{dest}}\rangle$  of the destination potential,  $V_{\text{dest}} = m\omega_0^2(\hat{x} - d)^2/2$  in a transporting time of  $T$ . We now look for a shortcut to the genuine state preparation by employing a mov-

ing harmonic potential with the same trap frequency  $\omega_0$ :  $V_{\text{move}}(t) = m\omega_0^2[\hat{x} - x_c(t)]^2/2$ , with the trajectory of the potential's center denoted as  $x_c(t)$ . It must satisfy the boundary conditions  $x_c(t < 0) = 0$  and  $x_c(t > T) = d$  to connect the initial and the destination potentials. The time-dependent Hamiltonian of the system can be expressed as

$$H(t) = \frac{\hat{p}^2}{2m} + V_{\text{move}}(t), \quad (1)$$

where  $\hat{p}$  denotes a momentum operator.

The ground state of a harmonic potential is a special coherent state with a minimal uncertainty in phase spaces ( $\Delta x \Delta p = \hbar/2$  and  $\Delta x(p) \equiv \hat{x}(\hat{p}) - \langle \hat{x}(\hat{p}) \rangle$ ), well-known for its shape-invariant wave-packet dynamics when it is displaced [43–45]. A coherent state  $|\alpha_0\rangle$  can be generated by applying a displacement operator  $\mathcal{D}(\alpha_0)$  to the ground state,  $|\alpha_0\rangle = \mathcal{D}(\alpha_0)|0\rangle$ , noting that  $\alpha_0$  is complex in general and its imaginary part corresponds to a momentum displacement. In a stationary potential, the complex amplitude can be expressed in dimensionless forms  $\alpha = \langle \hat{X} \rangle + i\langle \hat{P} \rangle$  with  $\hat{X} \equiv (\sqrt{m\omega_0/2\hbar})\hat{x}$  and  $\hat{P} \equiv \hat{p}/\sqrt{2\hbar m\omega_0}$ , and evolves as  $\alpha(t) = \alpha_0 e^{-i\omega_0 t}$ . In this phase space representation [46, 47], the Wigner function of a coherent state is a circularly symmetric Gaussian, and its evolution corresponds to a clockwise rotation around the origin, which is the center of the potential [49].

Role of the backward movement and the forward-moving speed limit—For a successful transport, we constrain the state evolution by the boundary conditions as required in evolving Eq. (1) toward the transport distance  $D \equiv (\sqrt{m\omega_0/2\hbar})d$  in a dimensionless form. First, the particle begins at rest ( $\langle \hat{X}(0) \rangle = \langle \hat{P}(0) \rangle = 0$ ), and the first potential move must be positive ( $X_1 > 0$ ) to initiate the coherent state evolution along the positive direction. On the other hand, the final step must ‘catch’ the state of the particle, bringing it to rest at the target ground state ( $\langle \hat{X}(T) \rangle = D, \langle \hat{P}(T) \rangle = 0$ ). This indicates that the state's center in phase spaces must evolve to the  $X$ -axis, without possessing any residual momentum. Therefore, the total accumulated angle of rotation during the transport is required to be a multiple of  $\pi$ , and the fastest process will correspond to the minimum angle, that is  $\theta = \pi$ . During this process, the momentum of the particle is always positive, and hence the final potential shift must also be a forward movement.

Notably, the opposite direction of the potential's movement affects this angular evolution in a favorable way. As shown in Fig. 1(a), a positive potential shift reduces the accumulated angle ( $\theta_2 < \theta_1$ ), which prolongs the evolution toward  $\pi$ . In contrast, a backward potential movement, shown in Fig. 1(b), increases the angle ( $\theta'_2 > \theta_1$ ) and accelerates the evolution due to  $X'_2 < X_1$ .

This insight immediately implies a speed limit for any transport protocol that uses only forward-moving poten-

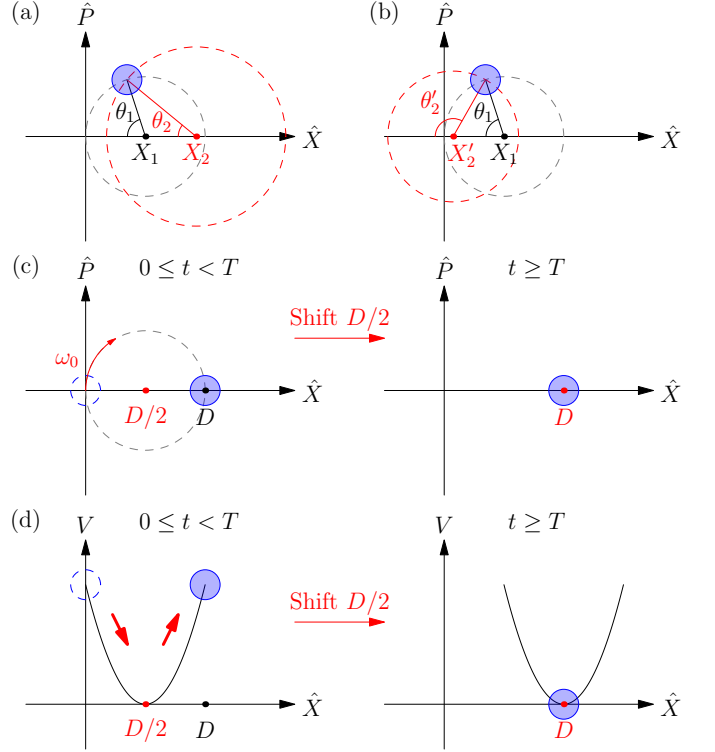


FIG. 1. A comparison of potential shift directions, forward or backward, on the phase-space evolution. Starting from an initial state at an angle  $\theta_1$  (when the potential is at  $X_1$ ), (a) a forward potential shift to  $X_2$  results in a new, smaller angle  $\theta_2$ . (b) By contrast, a backward shift to  $X'_2$  results in a new, larger angle  $\theta'_2$ . This illustrates the key finding that  $\theta_2 < \theta_1 < \theta'_2$ , demonstrating that forward movements inhibit while backward movements accelerate the angular evolution toward  $\pi$ . (c) Phase-space evolution and (d) the corresponding potential trajectory for the standard BB protocol, which demonstrate the forward-moving speed limit  $\tau_{\text{for}} = \pi/\omega_0$ . Dashed (filled) circles indicate the state of the particle at the beginning (end) of each free-evolution step.

tial shifts. Since every positive step slows the angular evolution, the fastest protocol using purely forward-moving potentials must be the one that minimizes these steps. The optimal protocol is a two-step process, known as a BB protocol [40, 41] as illustrated in Figs. 1(c,d). The potential is first shifted to  $D/2$ , displacing the particle and initiating the coherent state evolution. In a transport time  $T$ , the state fulfills the angle rotation of  $\pi$  and reaches the  $X$ -axis. At this moment, a second and instantaneous shift from  $D/2$  to  $D$  effectively catches the particle at the destination without extra momentum ( $\langle \hat{P} \rangle = 0$ ). Therefore, the time required for the transport of the BB protocol is  $T = \pi/\omega_0$ . This timescale represents the lower bound for any purely forward-moving transport:  $\tau_{\text{for}}(\omega) = \pi/\omega$ .

The BBB transport protocol—To further reduce the timescale set by the BB protocol, we employ a backward movement in the second ‘bang’ process of the BBB pro-

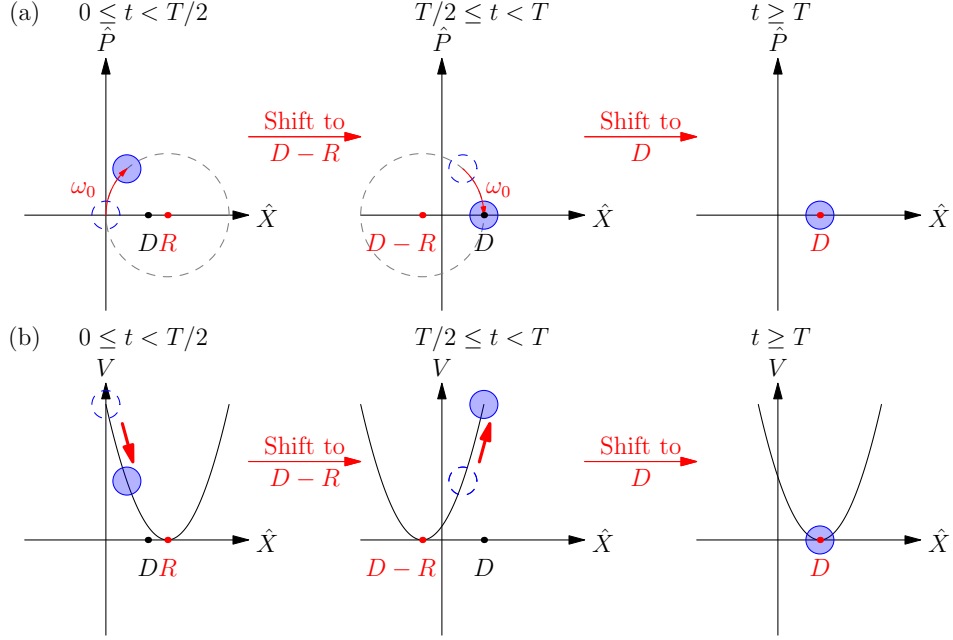


FIG. 2. The schematic of the BBB protocol. (a) The evolution of a coherent state in the space under the displaced potential with its center at  $R$  and  $D - R$ , respectively, in the first two bang processes of the BBB protocol, where the last bang process involves a shifted and holding potential at  $D$ . (b) The corresponding trajectory of the moving potential. The total transport time  $T \equiv \tau_{BBB}(\omega_0, R)$ . Dashed (filled) circles indicate the state at the beginning (end) of each free-evolution step.

tocol in Fig. 2, with the first and the last bang processes similar to the BB protocol. The trajectory of the center of the potential  $X_c^{BBB}$  is defined as

$$X_c^{BBB}(R, t) = \begin{cases} 0, & t < 0 \\ R, & 0 \leq t < \tau_{BBB}(R)/2 \\ D - R, & \tau_{BBB}(R)/2 \leq t < \tau_{BBB}(R) \\ D, & t \geq \tau_{BBB}(R) \end{cases} \quad (2)$$

where  $\tau_{BBB}(R)$  indicates the total transport time, depending on the parameter of dimensionless displacement  $R$ . The protocol is designed to be symmetric with respect to the midpoint  $D/2$ . At  $t = 0$ , the potential is shifted to  $R$ . The state evolves until  $t = \tau_{BBB}(R)/2$  when its position reaches  $\langle X \rangle = D/2$ . At this moment, a second bang is applied, shifting the potential to  $D - R$ , the position symmetric to  $R$  with respect to the midpoint. The state continues to evolve, and due to this symmetry in displacements, it arrives at the destination  $\langle X \rangle = D$  at  $t = \tau_{BBB}(R)$  with zero momentum ( $\langle P \rangle = 0$ ). The final bang process at  $t = \tau_{BBB}(R)$  shifts the potential to  $D$ , retaining the particle in the ground state of the destination potential.

The transport time for the BBB protocol can be calculated analytically, treating the trap frequency also as a parameter, which gives

$$\tau_{BBB}(\omega, R) = \frac{2}{\omega} \cos^{-1} \left( \frac{2R - D}{2R} \right). \quad (3)$$

The above solution also contains the results of forward-moving scenarios when  $R \leq D/2$ , where the case of  $R = D/2$  reduces the protocol to the standard BB protocol, that is  $\tau_{BBB}(\omega, D/2) = \pi/\omega$ , recovering the timescale for  $\tau_{\text{for}}$ . Notably, for any  $R > D/2$ , the second step  $D - R$  is less than  $D/2$ , constituting a backward movement. In this regime, the argument of the  $\cos^{-1}$  in Eq. (13) becomes positive, and the transport time  $\tau_{BBB}$  becomes shorter than  $\tau_{\text{for}}$ . Furthermore, in the limit of a large potential shift, the time approaches zero, that is  $\lim_{R \rightarrow \infty} \tau_{BBB}(R) = 0$ . This shows the ultimate timescale that should be limited by the quantum speed limit [1, 2, 30, 49, 52], which suggests an even better protocol than applying the conventional BB process.

The squeezed BBB (SBBB) protocol—For practical considerations, the potential is not perfectly harmonic. Its anharmonicity limits the effective confinement of the particle, leading to a restricted range of the parameter  $R$  in the BBB protocol. While the displacement  $R$  can be limited, the trap depth—and thus its trap frequency  $\omega$ —is highly controllable in systems like trapped ions and atoms in optical tweezers [48]. Therefore, we take  $\omega$  as a control parameter and adopt a squeezed coherent state evolution to further reduce the time for transport.

A simple and straightforward approach is to perform the entire BBB transport using a single, higher frequency  $\omega_1 > \omega_0$ . At  $t = 0$ , one would switch  $\omega_0 \rightarrow \omega_1$  and immediately begin the BBB protocol [see Fig. 3(a)]. The frequency switching squeezes the state's Wigner function

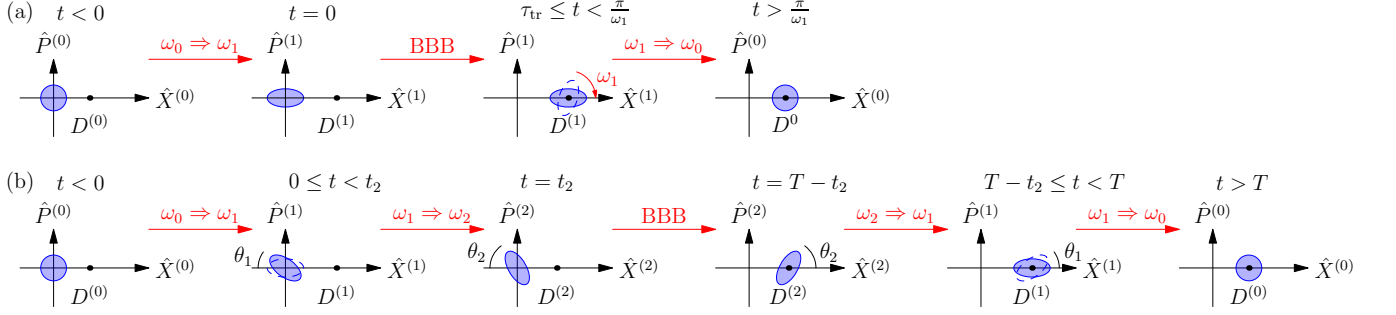


FIG. 3. Schematic of two squeezed-BBB (SBBB) protocols. (a) A single-frequency SBBB protocol using  $\omega_1$ . While the spacial transport (time  $\tau_{\text{tr}}$ ) can be made faster, the final squeezed state's orientation is mismatched with the target, requiring an extra wait time  $\tau_{\text{ex}}$  before the final re-squeeze. (b) The double-squeezed-BBB (DSBBB) protocol. Under the second squeeze ( $\omega_1 \rightarrow \omega_2$ ), the orientation angle becomes larger ( $\theta_2 > \theta_1$ ) when projected onto the trap potential with a smaller  $\omega_2 < \omega_1$ , accelerating the angular evolution. Dashed (filled) circles indicate the state at the beginning (end) of each free-evolution step. We define the dimensionless position, momentum, and destination with respect to the frequency  $\omega_i$  as  $\hat{X}^{(i)} \equiv (\sqrt{m\omega_i/2\hbar})\hat{x}$ ,  $\hat{P}^{(i)} \equiv \hat{p}/\sqrt{2\hbar m\omega_i}$ , and  $\hat{D}^{(i)} \equiv (\sqrt{m\omega_i/2\hbar})d$ , respectively.

from a circle into an ellipse in the phase spaces. The spatial transport of the ellipse's center becomes faster, as  $\tau_{\text{BBB}} \propto 1/\omega$ . However, to prepare the target ground state at the end of the whole protocol, this scheme takes an extra time of  $\tau_{\text{ex}}$  for the ellipse rotating to the correct orientation as its major axis overlaps with the  $X$ -axis. The whole process including the transport time  $\tau_{\text{tr}} = \tau_{\text{BBB}}(\omega_1, R)$  and  $\tau_{\text{ex}}$  are summed to be  $\pi/\omega_1$ , the same as the forward-moving speed limit  $\tau_{\text{for}}(\omega_1)$ . This indicates that the time for SBBB protocol is exactly the same as squeezed-BB (SBB) protocol when a single higher  $\omega_1$  is applied.

To further save the time for mismatched orientation, we propose a more sophisticated protocol, the double-squeezed-BBB (DSBBB), which can be illustrated in Fig. 3(b). The structure of the DSBBB protocol is similar to the BBB protocol, but it can facilitate the angle rotation by controlling the squeezed coherent state evolution. The key is to use a weaker intermediate trap frequency  $\omega_2 < \omega_1$  to compensate the extra time for state evolution, an issue in the SBBB protocol. This ultimately accelerates the overall ellipse rotations, just as a backward spatial move of  $D - R$  in Fig. 2 that speeds up the state transport. The DSBBB protocol proceeds as follows and in Fig. 3(b):

- Squeeze and wait: At  $t = t_1 = 0$ , we squeeze the state by applying  $\omega_0 \rightarrow \omega_1$  and wait for a time  $t_2$ . The angle of squeezed ellipse's orientation evolves, which can be tracked by the angle between its major axis and the  $X$ -axis as  $\theta_1 = \omega_1 t_2$ .
- Second squeeze: At  $t = t_2$ , we squeeze again using a smaller trap frequency  $\omega_2$  ( $\omega_1 \rightarrow \omega_2$ ). This suddenly changes the orientation angle from  $\theta_1$  to  $\theta_2$ .
- Slow angular evolution and BBB process: We then evolve the system under  $\omega_2$ . The ellipse's orientation angle accumulates at a frequency  $\omega_2$  from  $\theta_2$  to  $\pi - \theta_2$ , taking a time  $\tau_{\text{ori}} = [\pi - 2\theta_2(t_2)]/\omega_2$ . As the ellipse's

orientation evolves, the spatial transport by the BBB process is simultaneously performed, which takes a time  $\tau_{\text{BBB}}(\omega_2, R)$ . This transport time is required to be smaller than  $\tau_{\text{ori}}$  ( $\tau_{\text{BBB}} \leq \tau_{\text{ori}}$ ) to ensure that the subsequent re-squeezing process can be performed correctly.

(iv) Symmetric re-squeeze and wait: The process is then reversed symmetrically to the process (ii), where we squeeze the state back using  $\omega_2 \rightarrow \omega_1$  and wait for another time  $t_2$ .

(v) Final Squeeze: At  $t = T$ , we squeeze the trap frequency back to the initial stage of (i) as  $\omega_1 \rightarrow \omega_0$ .

The total time for this DSBBB protocol can be calculated as

$$\tau_{\text{DSBBB}}(\omega_1, \omega_2, t_2) = 2t_2 + \frac{\pi - 2\theta_2(t_2, \omega_1, \omega_2)}{\omega_2}, \quad (4)$$

under the condition  $\tau_{\text{BBB}}(\omega_2, R) \leq [\pi - 2\theta_2(t_2, \omega_1, \omega_2)]/\omega_2$  when  $\tau_{\text{ori}}$ , the second term of Eq. (4), is the dominating factor. We note that this condition can be released if we perform the BBB process starting from the beginning in Fig. 3(b), when two squeezing processes and spatial transport are conducted in parallel. This indicates that the condition  $\tau_{\text{BBB}} \leq \tau_{\text{DSBBB}}$  is sufficient to preserve the advantage of the DSBBB protocol, thereby relaxing the requirements on both the parameter  $R$  and the potential widths. In Fig. 4, we plot the difference between  $\tau_{\text{DSBBB}}$  and the transport time of the SBBB protocol using  $\omega_1$ , which is  $\pi/\omega_1$ . In this plot, we do not limit the range of the parameter  $R$  to satisfy the condition  $\tau_{\text{BBB}}(\omega_2, R) < [\pi - 2\theta_2(t_2, \omega_1, \omega_2)]/\omega_2$ . Figure 4 suggests that by choosing an appropriate squeezing time (blue area)  $t_1$  and  $\omega_2$  for a given  $\omega_1$ , the total transport time  $\tau_{\text{DSBBB}}$  can be made shorter than the simple SBBB protocol using only  $\omega_1$ . The speedup is feasible because the second squeeze is chosen to be a slower frequency ( $\omega_2 < \omega_1$ ), which leads to a beneficial jump in the orientation angle projection

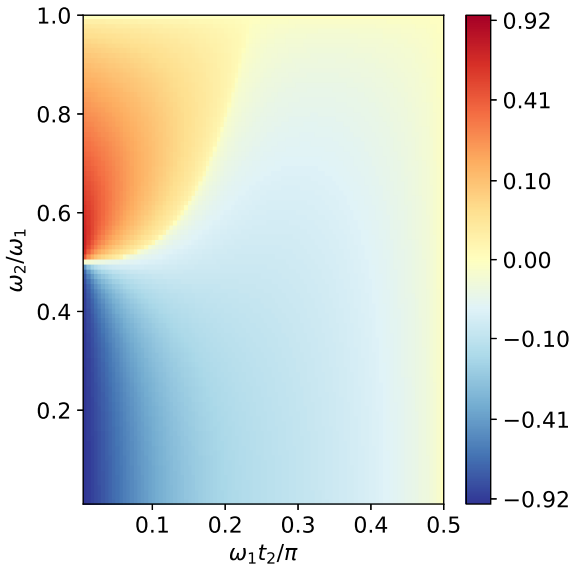


FIG. 4. Phase diagram of the time advantage,  $\tau_{\text{DSBBB}} - \pi/\omega_1$  (in units of  $\pi/\omega_1$ ), for the parameters of  $\omega_2$  and the first-squeeze time  $t_1$  at  $\omega_1 = 2\omega_0$ . The blue area shows where the DSBBA evolves faster than a straightforward SBBB protocol with a single  $\omega_1$ . The parameter space is plotted for  $\omega_2$  in the region  $(0, \omega_1]$  and  $t_2$  in the region  $(0, \pi/(2\omega_1)]$ . The range of  $t_2$  is bounded by  $\pi/(2\omega_1)$  in a symmetrical process within the time  $\pi/\omega_1$ .

( $\theta_2 > \theta_1$ ), accelerating the overall ellipse rotation. Note that the quantum speed limit emerges again as  $\omega_2$  and  $t_2$  approach zero, which is due to the significant jump of orientation angle projection in the DSBBA protocol [49].

Experimental feasibility—In trapped-ion platforms, it is already demonstrated that the BB control can be implemented to a coherent state with  $|\alpha| \approx 100$ , corresponding to displacing a  $^{40}\text{Ca}^+$  ion by  $1.49\mu\text{m}$  with a trap frequency of  $2.35\text{MHz}$  [40]. It is therefore promising that our proposed BBB protocol could be implemented in a similar experimental setup by controlling the harmonic potentials centered at  $R$  and  $D - R$  in Fig. 2. It is also possible to choose  $R = D$  for the ease of device design and fabrication. Assuming a similar allowable coherent state of  $|\alpha| \approx 100$ , our BBB protocol with  $R = D$  could transport a  $^{40}\text{Ca}^+$  ion a distance of  $0.785\mu\text{m}$  in two thirds of the time required by the standard BB protocol. By controlling the trap frequencies with assistance of squeezed coherent state evolution, it is expected to further reduce the transport time by adopting the DSBBA protocol. In other platforms like optical tweezers [53–59], the available controlled motional quanta might be lower (e.g.,  $|\alpha|^2 \approx 20$ ). The achievable distance for the BBB protocol, therefore, becomes smaller, but the general principle of accelerating transport by applying backward potential shifts in a continuous trajectory still remains feasible.

Conclusions and outlook—In this work, we propose an advanced bang-bang-bang protocol that can outperform the conventional forward-moving potential protocols by utilizing backward potential shifts. This provides an adaptable route to transport and prepare a coherent ground state with high fidelity reaching the quantum speed limit. Furthermore, we showcase the advantage of applying squeezed state evolution under a deeper followed by a weaker potential, which speeds up the state transport, surpassing the limitation set by the bang-bang-bang protocol. These protocols are promising for implementation in the trapped-ion and optical tweezer systems, providing a pathway to accelerating the speed of quantum computation and quantum information applications.

Extending our protocols to more realistic environments opens promising avenues for future research. Optimal quantum-control techniques [60, 61] or machine-learning approaches [62] may be explored for transporting atoms at finite temperatures [63, 64], where the trade-off between high-fidelity state preparation and transport time can be systematically investigated. Incorporating the effects of potential fluctuations due to electrical or laser-field noises, the finite switching time of instantaneous potential shifts [41], and experimentally relevant pulse shapes [65] will help determine the ultimate limits of transport performance—crucial for scalable atom-array architectures used in quantum simulation and quantum computation. Finally, manipulating locally squeezed coherent states offers a means to generate continuous-variable entanglement [66] in multi-ion systems, providing an alternative route toward quantum information processing.

Acknowledgments—We acknowledge support from the National Science and Technology Council (NSTC), Taiwan, under the Grants No. 112-2112-M-001-079-MY3 and No. NSTC-114-2119-M-001-005, and from Academia Sinica under Grant AS-CDA-113-M04. We are also grateful for support from TG 1.2 of NCTS at NTU.

Data Availability—The data are available from the authors upon reasonable request.

\* yatan1018@gmail.com

† sappyjen@gmail.com

- [1] M. A. Nielsen and I. L. Chuang. *Quantum Computation and Quantum Information*, Cambridge University Press (2000).
- [2] J. I. Cirac and P. Zoller, Quantum Computations with Cold Trapped Ions, *Phys. Rev. Lett.* 74, 4091 (1995).
- [3] D. Kielpinski, C. Monroe and D. Wineland, Architecture for a large-scale ion-trap quantum computer, *Nature* 417, 709–711 (2002).
- [4] D. Leibfried, R. Blatt, C. Monroe, and D. Wineland, Quantum dynamics of single trapped ions, *Rev. Mod. Phys.* 75, 281 (2003).

[5] H. Häffner, C. Roos, and R. Blatt, Quantum computing with trapped ions, *Phys. Rep.* 469, 155 (2008).

[6] J. P. Home, D. Hanneke, J. D. Jost, J. M. Amini, D. Leibfried, and D. J. Wineland, Complete Methods Set for Scalable Ion Trap Quantum Information Processing, *Science* 325, 1227 (2009).

[7] H.-Y. Lo, D. Kienzler, L. de Clercq, M. Marinelli, V. Negnevitsky, B. C. Keitch, and J. P. Home, Spin-motion entanglement and state diagnosis with squeezed oscillator wavepackets, *Nature* 521, 336 (2015).

[8] D. Bluvstein, H. Levine, G. Semeghini, T. T. Wang, S. Ebadi, M. Kalinowski, A. Keesling, N. Maskara, H. Pichler et al., A quantum processor based on coherent transport of entangled atom arrays, *Nature* 604, 451 (2022).

[9] T. M. Graham, Y. Song, J. Scott, C. Poole, L. Phuttitarn, K. Jooya, P. Eichler, X. Jiang, A. Marra et al., Multi-qubit entanglement and algorithms on a neutral-atom quantum computer, *Nature* 604, 457 (2022).

[10] S. Jandura and G. Pupillo, Time-Optimal Two- and Three-Qubit Gates for Rydberg Atoms, *Quantum* 6, 712 (2022).

[11] S. A. Moses, C. H. Baldwin, M. S. Allman, R. Ancona, L. Ascarrunz, C. Barnes, J. Bartolotta, B. Bjork, P. Blanchard et al., A Race-Track Trapped-Ion Quantum Processor, *Phys. Rev. X* 13, 041052 (2023).

[12] S. J. Evered, D. Bluvstein, M. Kalinowski, S. Ebadi, T. Manovitz, H. Zhou, S. H. Li, A. A. Geim, T. T. Wang et al., High-fidelity parallel entangling gates on a neutral-atom quantum computer, *Nature* 622, 268 (2023).

[13] T. H. Chang, T. N. Wang, H. H. Jen, and Y.-C. Chen, High-fidelity Rydberg controlled-Z gates with optimized pulses, *New J. phys.* 25, 123007 (2023).

[14] D. Bluvstein, S. J. Evered, A. A. Geim, S. H. Li, H. Zhou, T. Manovitz, S. Ebadi, M. Cain, M. Kalinowski et al., Logical quantum processor based on reconfigurable atom arrays, *Nature* 626, 58 (2024).

[15] H. J. Manetsch, G. Nomura, E. Bataille, X. Lv, K. H. Leung, and M. Endres, A tweezer array with 6,100 highly coherent atomic qubits, *Nature* 647, 60 (2025).

[16] D. J. Wineland, C. Monroe, W. M. Itano, D. Leibfried, B. E. King, and D. M. Meekhof, J. Res, Experimental Issues in Coherent Quantum-State Manipulation of Trapped Atomic Ions, *Natl. Inst. Stand. Technol. Rev.* 103, 259 (1998).

[17] A. S. Parkins and H. J. Kimble, Quantum state transfer between motion and light, *J. Opt. B: Quantum Semiclassical Opt.* 1, 496 (1999).

[18] M. A. Rowe et al, Transport of quantum states and separation of ions in a dual RF ion trap. *Quant. Inform. Comput.* 2, 257–271 (2002).

[19] R. Reichle, D. Leibfried, R.B. Blakestad, J. Britton, J.D. Jost, E. Knill, C. Langer, R. Ozeri, S. Seidelin, D.J. Wineland, Transport dynamics of single ions in segmented microstructured Paul trap arrays, *Fortschr. Phys.* 54, 666 (2006).

[20] R. Bowler, et al, Coherent diabatic ion transport and separation in a multizone trap array. *Phys. Rev. Lett.* 109, 080502 (2012).

[21] D. Guéry-Odelin, A. Ruschhaupt, A. Kiely, E. Torrontegui, S. Martínez-Garaot, and J. G. Muga, Shortcuts to adiabaticity: Concepts, methods, and applications, *Rev. Mod. Phys.* 91, 045001 (2019).

[22] X. Chen, A. Ruschhaupt, S. Schmidt, A. del Campo, D. Guéry-Odelin, and J. G. Muga, Fast Optimal Frictionless Atom Cooling in Harmonic Traps: Shortcut to Adiabaticity, *Phys. Rev. Lett.* 104, 063002 (2010).

[23] S. An, D. Lv, A. del Campo, and K. Kim, Shortcuts to adiabaticity by counterdiabatic driving for trapped-ion displacement in phase space, *Nat. Commun.* 7, 12999 (2016).

[24] P. Kaufmann, T. F. Gloer, D. Kaufmann, M. Johanning, and C. Wunderlich, High-Fidelity Preservation of Quantum Information During Trapped-Ion Transport, *Phys. Rev. Lett.* 120, 010501 (2018).

[25] J. R. Finžgar, S. Notarnicola, M. Cain, M. D. Lukin, and D. Sels, Counterdiabatic Driving with Performance Guarantees, *Phys. Rev. Lett.* 135, 180602 (2025).

[26] M. Murphy, L. Jiang, N. Khaneja, and T. Calarco, High-Fidelity Fast Quantum Transport with Imperfect Controls, *Phys. Rev. A* 79, 020301(R) (2009).

[27] X. Chen, E. Torrontegui, D. Stefanatos, J.-S. Li, and J. G. Muga, Optimal trajectories for efficient atomic transport without final excitation, *Phys. Rev. A* 84, 043415, (2011).

[28] E. Torrontegui, S. Ibáñez, X. Chen, A. Ruschhaupt, D. Guéry-Odelin, and J. G. Muga, Fast Atomic Transport without Vibrational Heating, *Phys. Rev. A* 83, 013415 (2011).

[29] Y. Ding, T.-Y. Huang, K. Paul, M. Hao, and X. Chen, Smooth bang-bang shortcuts to adiabaticity for atomic transport in a moving harmonic trap, *Phys. Rev. A* 101, 063410, (2020).

[30] M. R. Lam, N. Peter, T. n Groh, W.g Alt, C. Robens, D. Meschede, A. Negretti, S. Montangero, T. Calarco et al., Demonstration of Quantum Brachistochrones between Distant States of an Atom, *Phys. Rev. X* 11, 011035 (2021).

[31] S. Hwang, H. Hwang, K. Kim, A. Byun, K. Kim, S. Jeong, M. P. Soegianto, and J. Ahn, Fast and reliable atom transport by optical tweezers, *Optica Quantum* 3, 64 (2025).

[32] G. S. Agarwal, Brownian Motion of a Quantum Oscillator, *Phys. Rev. A* 4, 739 (1971).

[33] D. J. Daniel and G. J. Milburn, Destruction of quantum coherence in a nonlinear oscillator via attenuation and amplification, *Phys. Rev. A* 39, 4628 (1989).

[34] D. J. Wineland, C. Monroe, W. M. Itano, D. Leibfried, B. E. King, D. M. Meekhof, Experimental Issues in Coherent Quantum-State Manipulation of Trapped Atomic Ions, *J. Res. Natl. Inst. Stand. Technol. Rev.* 103, 259 (1998).

[35] Z. Zhang, M. Yuan, B. Sundar, and K. R. A. Hazzard, Motional decoherence in ultracold-Rydberg-atom quantum simulators of spin models, *Phys. Rev. A* 110, 053321 (2024).

[36] D. J. Wineland, C. Monroe, D. M. Meekhof, B. E. King, D. Leibfried, W. M. Itano, J. C. Bergquist, D. Berkeland, J. J. Bollinger and J. Miller, Quantum state manipulation of trapped atomic ions, *Proc. Roy. Soc. A* 454, 1969 (1998).

[37] L. Viola, E. Knill and S. Lloyd, Dynamical decoupling of open quantum systems. *Phys. Rev. Lett.* 82, 2417–2421 (1999).

[38] J. J. Morton, et al, Bang-bang control of fullerene qubits using ultrafast phase gates. *Nat. Phys.* 2, 40–43 (2006).

[39] S. Damodarakurup, M. Lucamarini, G. Di Giuseppe, D. Vitali and P. Tombesi, Experimental inhibition of decoherence on flying qubits via ‘bang-bang’ control. *Phys. Rev. Lett.* 103, 040502 (2009).

[40] J. Alonso, F. M. Leupold, Z. U. Solèr, M. Fadel, M. Marinelli, B. C. Keitch, V. Negnevitsky and J.P. Home,

Generation of large coherent states by bang–bang control of a trapped-ion oscillator, *Nat Commun* 7, 11243 (2016).

[41] J. Alonso, F. M. Leupold, B. C. Keitch and J. P. Home, Quantum control of the motional states of trapped ions through fast switching of trapping potentials, *New J. Phys.* 15 023001 (2013).

[42] D. F. Walls, Squeezed states of light, *Nature* 306, 141 (1983).

[43] E. C. G. Sudarshan, Equivalence of Semiclassical and Quantum Mechanical Descriptions of Statistical Light Beams, *Phys. Rev. Lett.* 10, 277 (1963).

[44] R. J. Glauber, Coherent and Incoherent States of the Radiation Field, *Phys. Rev.* 131, 2766 (1963).

[45] W.-M. Zhang, D. H. Feng, and R. Gilmore, Coherent states: Theory and some applications, *Rev. Mod. Phys.* 62, 867 (1990).

[46] E. Wigner, On the Quantum Correction for Thermodynamic Equilibrium, *Phys. Rev.* 40, 749 (1932).

[47] M. O. Scully and M. S. Zubairy, *Quantum Optics*, Cambridge University Press (1997).

[48] J. Beugnon, C. Tuchendler, H. Marion, A. Gaëtan, Y. Miroshnychenko, Y. R. P. Sortais, A. M. Lance, M. P. A. Jones, G. Messin et al., Two-dimensional transport and transfer of a single atomic qubit in optical tweezers, *Nat. Phys.* 3, 696 (2007).

[49] See supplemental material for details of the evolution of a coherent state under a series of potential shifts, the quantum speed limit, and the calculation of the orientation angle for the squeezed coherent state.

[50] L. Mandelstam and I. Tamm, The Uncertainty Relation between Energy and Time in Non-Relativistic Quantum Mechanics, *J. Phys. (Moscow)* 9, 249 (1945).

[51] N. Margolus and L. B. Levitin, The maximum speed of dynamical evolution, *Physica (Amsterdam)* 120D, 188 (1998).

[52] G. Ness, A. Alberti and Y. Sagi, Quantum Speed Limit for States with a Bounded Energy Spectrum, *Phys. Rev. Lett.* 129, 140403 (2022).

[53] A. M. Kaufman, B. J. Lester, and C. A. Regal, Cooling a Single Atom in an Optical Tweezer to Its Quantum Ground State, *Phys. Rev. X* 2, 041014 (2012).

[54] D. Barredo, S. de Léséleuc, V. Lienhard, T. Lahaye, and A. Browaeys, An atom-by-atom assembler of defect-free arbitrary two-dimensional atomic arrays, *Science* 354, 1021 (2016).

[55] D. Barredo, V. Lienhard, S. de Léséleuc, T. Lahaye, and A. Browaeys, Synthetic three-dimensional atomic structures assembled atom by atom, *Nature* 561, 79 (2018).

[56] M. O. Brown, T. Thiele, C. Kiehl, T.-W. Hsu, and C. A. Regal, Gray-Molasses Optical-Tweezer Loading: Controlling Collisions for Scaling Atom-Array Assembly, *Phys. Rev. X* 9, 011057 (2019).

[57] S. Ebadi, T. T. Wang, H. Levine, A. Keesling, G. Saghini, A. Omran, D. Bluvstein, R. Samajdar et al., Quantum phases of matter on a 256-atom programmable quantum simulator, *Nature* 595, 227 (2021).

[58] P. Scholl, M. Schuler, H. J. Williams, A. A. Eberharter, D. Barredo, K.-N. Schymik, V. Lienhard, L.-P. Henry, T. C. Lang et al., Quantum simulation of 2D antiferromagnets with hundreds of Rydberg atoms, *Nature* 595, 233 (2021).

[59] T. Dordević, P. Samutpraphoot, P. L. Ocola, H. Bernien, B. Grinkemeyer, I. Dimitrova, V. Vuletić, and M. D. Lukin, Entanglement transport and a nanophotonic interface for atoms in optical tweezers, *Science* 373, 1511 (2021).

[60] T. Caneva, M. Murphy, T. Calarco, R. Fazio, S. Montangero, V. Giovannetti, and G. E. Santoro, Optimal control at the quantum speed limit, *Phys. Rev. Lett.* 103, 240501 (2009).

[61] H. A. Fürst, M. H. Goerz, U. G. Poschinger, M. Murphy, S. Montangero, T. Calarco, F. Schmidt-Kaler, K. Singer, and C. P. Koch, Controlling the transport of an ion: Classical and quantum mechanical solutions, *New J. Phys.* 16, 075007 (2014).

[62] X.-M. Zhang, Z.-W. Cui, X. Wang, and M.-H. Yung, Automatic spin-chain learning to explore the quantum speed limit, *Phys. Rev. A* 97, 052333 (2018).

[63] A. Pagano, D. Jaschke, W. Weiss, and S. Montangero, Optimal control transport of neutral atoms in optical tweezers at finite temperature, *Phys. Rev. Res.* 6, 033282 (2024).

[64] O. Morandi, S. Nicoletti, V. Gavryusev, and L. Fallani, Optimal control in phase space applied to minimal-time transfer of thermal atoms in optical traps, *Phys. Rev. A* 111, 063312 (2025).

[65] C. Cicali, M. Calzavara, E. Cuestas, T. Calarco, R. Zeier, and F. Motzoi, Fast neutral-atom transport and transfer between optical tweezers, *Phys. Rev. Appl.* 24, 024070 (2025).

[66] A. Serafini, A. Retzker and M. B. Plenio, Manipulating the quantum information of the radial modes of trapped ions: linear phononics, entanglement generation, quantum state transmission and non-locality tests, *New. J. Phys.* 11, 023007 (2009).

---

#### SUPPLEMENTARY INFORMATION:

AN ADAPTABLE ROUTE TO FAST COHERENT STATE TRANSPORT VIA BANG–BANG–BANG PROTOCOLS

#### Coherent State Evolution under a Stepwise Potential Trajectory

We consider an  $N$ -step trajectory  $X_c^N(t)$  for a moving harmonic potential. The potential traps a particle of mass  $m$  with a constant trap frequency  $\omega_0$ . The trajectory, expressed in the dimensionless  $\hat{X} - \hat{P}$  coordinate system, is

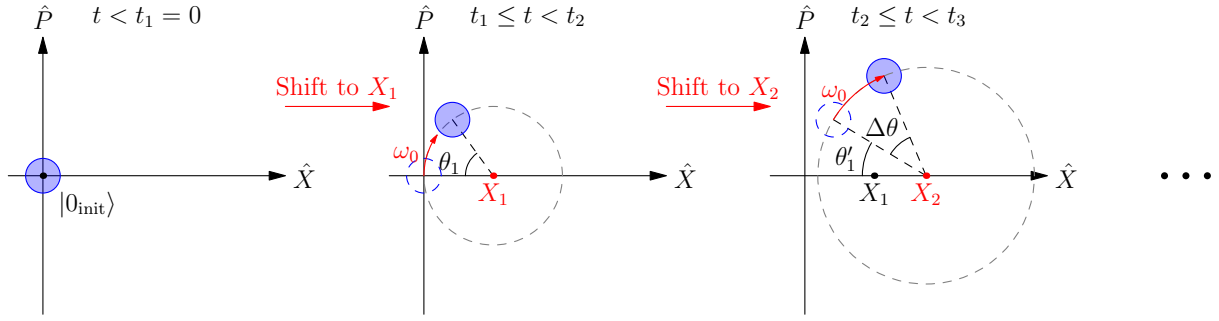


FIG. 5. Phase-space evolution of a coherent state under an  $N$ -step moving potential. The state begins at the origin (the ground state  $|0_{\text{init}}\rangle$ ). At  $t_1 = 0$ , the potential shifts to  $X_1$ , causing the state to rotate around  $(X_1, 0)$  until  $t_2$ . At  $t_2$ , the potential shifts to  $X_2$ , and the state's center of rotation switches to  $(X_2, 0)$ , continuing until  $t_3$ . This process repeats for all subsequent steps until  $t = T$ . Dashed (filled) circles indicate the coherent state at the beginning (end) of each free-evolution step.

given by:

$$X_c^N(t) = \begin{cases} 0, & t < t_1 = 0 \\ X_1, & t_1 \leq t < t_2 \\ \vdots & \\ X_i, & t_i \leq t < t_{i+1} \\ \vdots & \\ X_{N-1}, & t_{N-1} \leq t < t_N \\ D, & t \geq t_N = T \end{cases}, \quad (5)$$

The dimensionless coordinates are defined as  $\hat{X} \equiv (\sqrt{m\omega_0/2\hbar})\hat{x}$  (position) and  $\hat{P} \equiv \hat{p}/\sqrt{2\hbar m\omega_0}$  (momentum), where  $\hat{x}$  and  $\hat{p}$  are the position and momentum operators. The total transport distance  $d$  is represented by the dimensionless quantity  $D = (\sqrt{m\omega_0/2\hbar})d$ . In the trajectory,  $X_i$  is the potential's center at step  $i$ ,  $t_i$  is the time of the  $i$ -th potential shift, and  $T = t_N$  is the total transport time.

The evolution of a coherent state in phase space under this kind of discrete potential trajectory consists of a series of clockwise rotations. We visualize the first two steps in Fig. 5, and the process is described as follows:

- (i) Initially, the particle begins at the ground state of the initial potential, corresponding to the initial condition ( $\langle X(0) \rangle = \langle P(0) \rangle = 0$ ).
- (ii) At  $t = t_1 = 0$ , the potential suddenly shifts to  $X_1$ . The coherent state then begins to rotate clockwise around the point  $(X_1, 0)$  with angular frequency  $\omega_0$ .
- (iii) The rotation continues until  $t = t_2$ , accumulating a phase angle  $\theta_1 = \omega_0 t_2$ .
- (iv) At  $t = t_2$ , the potential shifts again to  $X_2$ . The state's center of rotation instantly switches to  $(X_2, 0)$ , and it begins to rotate around this new point.
- (v) The rotation continues until  $t = t_3$ , accumulating a further angle  $\Delta\theta = \omega_0(t_3 - t_2)$ .
- (vi) This process is repeated for all subsequent steps. At the final step ( $t = t_N = T$ ), the potential shifts to  $D$  and remains there, 'catching' the particle at the destination as the ground state.

### Quantum Speed Limit Analysis of the Bang-Bang-Bang Protocol

The minimal time for a quantum evolution is constrained by the Quantum Speed Limit (QSL). Two of the most fundamental bounds are those proposed by Mandelstam and Tamm (MT) [1] and Margolus and Levitin (ML) [2]. For a transition between an initial state  $|\psi_{\text{init}}\rangle$  and a target state  $|\psi_{\text{targ}}\rangle$ , these bounds are given by

$$\tau_{\text{MT}} = \frac{\hbar}{\Delta E} \cos^{-1} (|\langle \psi_{\text{init}} | \psi_{\text{targ}} \rangle|), \quad (6)$$

$$\tau_{\text{ML}} = \frac{\hbar}{E} \cos^{-1} (|\langle \psi_{\text{init}} | \psi_{\text{targ}} \rangle|), \quad (7)$$

where  $E$  is the time averaged mean energy (relative to the ground state), and  $\Delta E$  is the time averaged energy spread (standard deviation).

For a transport process,  $|\psi_{\text{init}}\rangle$  is the ground state of the initial potential, and  $|\psi_{\text{targ}}\rangle$  is the ground state  $|\psi_{\text{dest}}\rangle$  of the destination potential, which is displaced by a distance  $d$ . The overlap between these two harmonic oscillator ground states (for a particle of mass  $m$  at frequency  $\omega_0$ ) is

$$|\langle \psi_{\text{init}} | \psi_{\text{dest}} \rangle| = \exp \left[ -\frac{m\omega_0 d^2}{4\hbar} \right] = \exp \left[ -\frac{D^2}{2} \right]. \quad (8)$$

For a realistic transport, we assume the dimensionless distance  $D$  is large enough (e.g.,  $D \approx 3$ , where the overlap is around 1%) that the states are nearly orthogonal, which gives  $\cos^{-1}(0) \approx \pi/2$ .

For our Bang-Bang-Bang (BBB) protocol, the coherent state excitation is set by the parameter  $R$ , which corresponds to the initial dimensionless potential displacement used in the protocol. This results in a coherent state of magnitude  $|\alpha| = R$ , and for the whole BBB process, this magnitude remains invariant. For a coherent state in a quantum harmonic oscillator, the mean energy (relative to the ground state energy) is given by

$$E \equiv \langle H \rangle - E_0 = \hbar\omega_0|\alpha|^2, \quad (9)$$

and the energy spread (the standard deviation of energy) is

$$\Delta E \equiv (\langle H^2 \rangle - \langle H \rangle^2)^{1/2} = \hbar\omega_0|\alpha|, \quad (10)$$

where  $H$  is the Hamiltonian of the harmonic oscillator. Substituting  $|\alpha| = R$  into the QSLs with the  $\pi/2$  orthogonality approximation, we find the bounds for the BBB protocol, which are

$$\tau_{\text{MT}}^{\text{BBB}}(R) \approx \frac{\pi}{2R\omega_0}, \quad (11)$$

$$\tau_{\text{ML}}^{\text{BBB}}(R) \approx \frac{\pi}{2R^2\omega_0}. \quad (12)$$

The transport time of the BBB protocol (at frequency  $\omega_0$ ) is

$$\tau_{\text{BBB}}(R) = \frac{2}{\omega_0} \cos^{-1} \left( 1 - \frac{D}{2R} \right). \quad (13)$$

In Fig. 6, we plot these three timescales as a function of  $R$ .  $\tau_{\text{BBB}}$  clearly remains above both QSL bounds for finite  $R$ . In the limit  $R \rightarrow \infty$ , we can expand the inverse cosine function in Eq. 13 into a Puiseux series, where

$$\cos^{-1}(1 - x) = \sqrt{2x} \left( 1 + \frac{1}{12}x + \mathcal{O}(x^2) \right). \quad (14)$$

This gives the asymptotic behavior of the BBB time as

$$\tau_{\text{BBB}}(R \rightarrow \infty) \approx \frac{2}{\omega_0} \sqrt{2 \left( \frac{D}{2R} \right)} = \frac{2\sqrt{D}}{\omega_0\sqrt{R}}. \quad (15)$$

Since  $\sqrt{R}$  scales slower than  $R$ , our protocol time  $\tau_{\text{BBB}} \propto 1/\sqrt{R}$  is well above the MT bound  $\tau_{\text{MT}} \propto 1/R$  and the ML bound  $\tau_{\text{ML}} \propto 1/(R)^2$  for large  $R$ .

Our analysis confirms that  $\tau_{\text{BBB}}$  does not violate these two fundamental QSLs. This result suggests that either (i) an even faster protocol may exist that more closely approaches these limits, or (ii) a different QSL, one more specific to transport protocols, could provide a tighter bound for this setup.

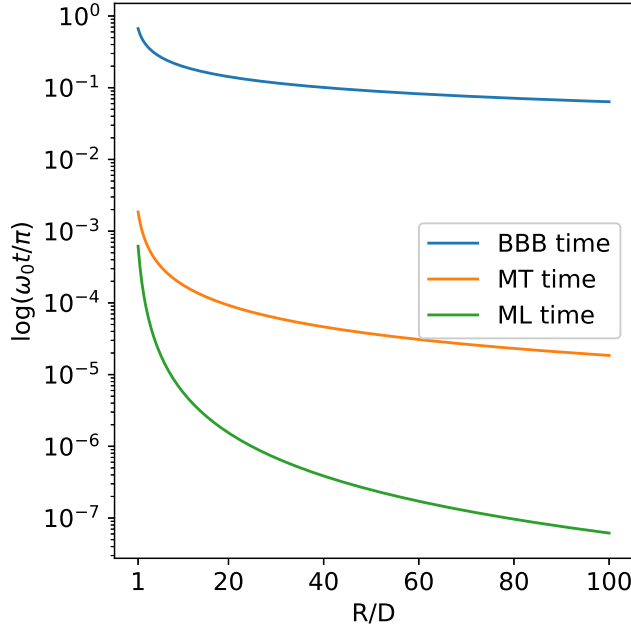


FIG. 6. Timescales with respect to the parameter  $R$  over the range  $[D, 100D]$ . The blue line is the BBB transport time  $\tau_{\text{BBB}}$ , while the orange and green lines show the MT bound  $\tau_{\text{MT}}$  and the ML bound  $\tau_{\text{ML}}$ , respectively. For finite  $R$ ,  $\tau_{\text{BBB}}$  is always larger than  $\tau_{\text{MT}}$  and  $\tau_{\text{ML}}$ , which shows that BBB protocol does not violate the fundamental principles of quantum mechanics.

#### The Major Axis Orientation of the Squeezed State

When the trap frequency  $\omega$  is changed, a coherent state is squeezed. The Wigner function of a state in a harmonic potential with frequency  $\omega$  undergoes shape-preserving clockwise rotation in the appropriate phase space. Therefore, to correctly analyze the dynamics, we must use a coordinate system scaled by the corresponding frequency. We define the  $\hat{X}^{(i)} - \hat{P}^{(i)}$  coordinate system for a frequency  $\omega_i$  as

$$\hat{X}^{(i)} = (\sqrt{m\omega_i/2\hbar})\hat{x} \quad \text{and} \quad \hat{P}^{(i)} = \hat{p}/\sqrt{2\hbar m\omega_i}. \quad (16)$$

In this section, we explain the details of the mapping between these coordinate systems to track the major axis orientation of the squeezed coherent state. Fig. 7 visualizes the transformations explained in the following contents. First Squeeze and Rotation

Initially, a standard coherent state is prepared in the harmonic potential with trap frequency  $\omega_0$ . Its Wigner function is a circularly symmetric Gaussian in the  $\hat{X}^{(0)} - \hat{P}^{(0)}$  phase space [Fig. 7(a)].

At  $t = t_1 = 0$ , the frequency suddenly changes to  $\omega_1$ . The coordinates are transformed from the  $\hat{X}^{(0)} - \hat{P}^{(0)}$  system to the  $\hat{X}^{(1)} - \hat{P}^{(1)}$  system by the matrix

$$S_0^1 = \begin{pmatrix} \sqrt{\omega_1/\omega_0} & 0 \\ 0 & \sqrt{\omega_0/\omega_1} \end{pmatrix}. \quad (17)$$

This transforms the initial circle into an ellipse [Fig. 7(b)]. If  $\omega_1 > \omega_0$ , the ellipse is ‘flat’ (squeezed in momentum); if  $\omega_1 < \omega_0$ , it is ‘thin’ (squeezed in position). We define the initial principal semi-axis vectors (which correspond to the 1-sigma uncertainties) as

$$\vec{a}_0 = (\frac{1}{2}\sqrt{\omega_1/\omega_0}, 0) \quad \text{and} \quad \vec{b}_0 = (0, \frac{1}{2}\sqrt{\omega_0/\omega_1}). \quad (18)$$

Their lengths represent the uncertainties  $|\vec{a}_0| \equiv \Delta X^{(1)}$  and  $|\vec{b}_0| \equiv \Delta P^{(1)}$ , which fulfill the minimum uncertainty relation  $\Delta X^{(1)}\Delta P^{(1)} = 1/4$ . As time evolves, the ellipse rotates clockwise at frequency  $\omega_1$ . At time  $t_2$ , the accumulated angle is  $\theta_1 = \omega_1(t_2 - t_1)$  [Fig. 7(c)]. The two axis vectors are transformed by the clockwise rotation matrix  $R(\theta_1)$  as

$$\vec{a}_1 = R(\theta_1)\vec{a}_0 \quad \text{and} \quad \vec{b}_1 = R(\theta_1)\vec{b}_0, \quad (19)$$

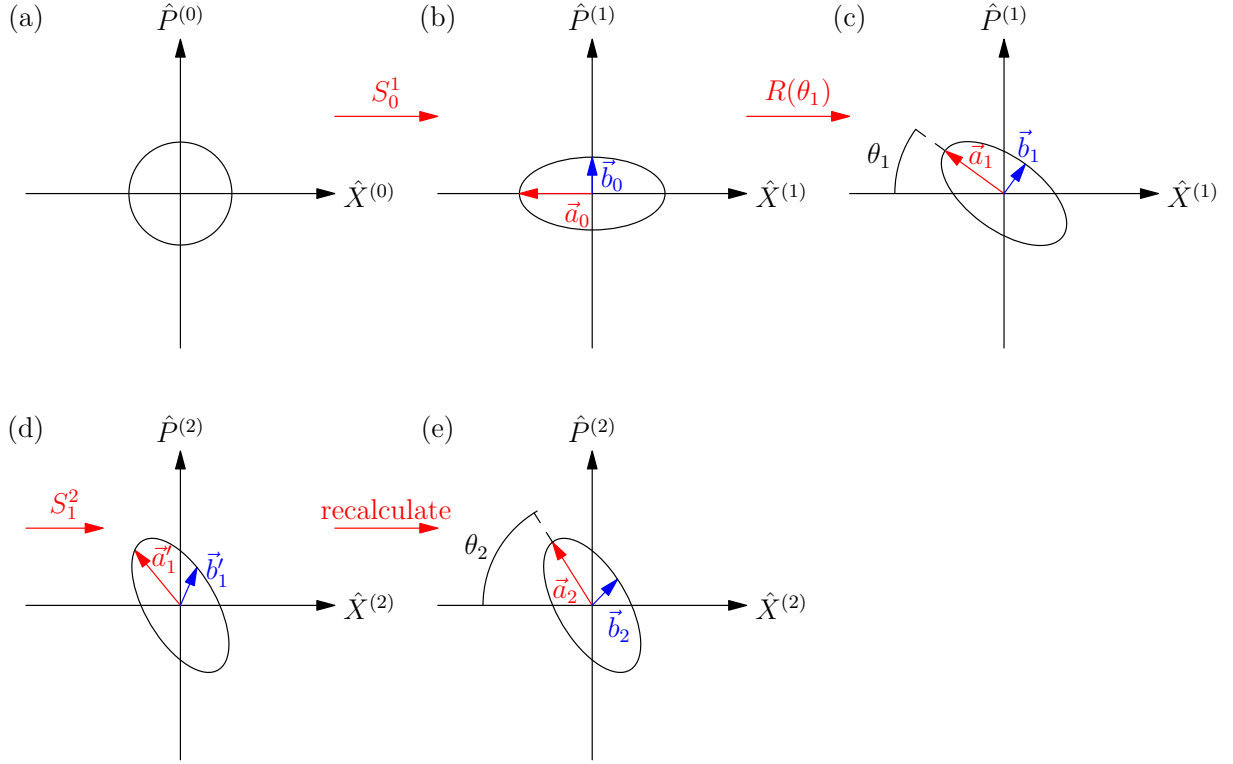


FIG. 7. The transformations of the semi-major and semi-minor axes. (a) The particle is initially a standard coherent state, which is a circle in the  $\hat{X}^{(0)} - \hat{P}^{(0)}$  phase space. (b) At  $t = t_1 = 0$ , a sudden change of trap frequency  $\omega_0 \rightarrow \omega_1$  squeezes the state into an ellipse in the  $\hat{X}^{(1)} - \hat{P}^{(1)}$  phase space. (c) The ellipse rotates, accumulating an orientation angle of  $\theta_1 = \omega_1 t_2$ . (d) At  $t = t_2$ , the frequency changes again ( $\omega_1 \rightarrow \omega_2$ ), but the transformed vectors  $\vec{a}'_1$  and  $\vec{b}'_1$  are not the new semi-major/minor axes. (e) The new principal axes are recalculated to compute  $\theta_2$ . The black circles/ellipses show the 1-sigma contour of the standard/squeezed coherent states.

where

$$R(\theta_1) = \begin{pmatrix} \cos \theta_1 & \sin \theta_1 \\ -\sin \theta_1 & \cos \theta_1 \end{pmatrix}. \quad (20)$$

#### Second Squeeze and New Axis Calculation

At  $t = t_2$ , the second squeeze is performed ( $\omega_1 \rightarrow \omega_2$ ). We map the state into the  $\hat{X}^{(2)} - \hat{P}^{(2)}$  coordinate system using the matrix

$$S_1^2 = \begin{pmatrix} \sqrt{\omega_2/\omega_1} & 0 \\ 0 & \sqrt{\omega_1/\omega_2} \end{pmatrix}. \quad (21)$$

Applying this transform to the rotated axes gives  $\vec{a}'_1 = S_1^2 \vec{a}_1$  and  $\vec{b}'_1 = S_1^2 \vec{b}_1$  [Fig. 7(d)]. A problem occurs: because  $S_1^2$  is a squeezing operation (not a simple rotation), these new vectors  $\vec{a}'_1$  and  $\vec{b}'_1$  are no longer orthogonal and do not represent the semi-major/minor axes of the new ellipse. We must find the new principal axes. The points on the new ellipse (which was the 1-sigma contour) can be parametrized by  $\phi$

$$\vec{v}(\phi) = \cos(\phi) \vec{a}'_1 + \sin(\phi) \vec{b}'_1. \quad (22)$$

The semi-major and semi-minor axes correspond to the extrema of the distance  $|\vec{v}(\phi)|$ . These occur at angles  $\alpha$  and  $\beta$  where the derivative  $d/d\phi [|\vec{v}(\phi)|^2]|_{\phi=\alpha,\beta} = 0$ . This calculation yields the condition for the extrema angles

$$\tan(2\alpha) = \frac{2\vec{a}'_1 \cdot \vec{b}'_1}{|\vec{a}'_1|^2 - |\vec{b}'_1|^2}. \quad (23)$$

Substituting the two resulting angles into Eq. (22) gives the new semi-major and semi-minor axis vectors,  $\vec{a}_2$  and  $\vec{b}_2$

$$\vec{a}_2 = \cos(\alpha)\vec{a}'_1 + \sin(\alpha)\vec{b}'_1 \quad (24)$$

$$\vec{b}_2 = \cos(\beta)\vec{a}'_1 + \sin(\beta)\vec{b}'_1. \quad (25)$$

Finally, we can calculate the new orientation angle  $\theta_2$  of the semi-major axis  $\vec{a}_2$  in the  $\hat{X}^2 - \hat{P}^2$  coordinate system [Fig. 7(e)]. If the new major axis vector is  $\vec{a}_2 = (a_2^x, a_2^p)$ , the angle is given by:

$$\theta_2 = \tan^{-1}(-a_2^p/a_2^x). \quad (26)$$

---

<sup>\*</sup> yatan1018@gmail.com

<sup>†</sup> sappyjen@gmail.com

[1] L. Mandelstam and I. Tamm, The Uncertainty Relation between Energy and Time in Non-Relativistic Quantum Mechanics, *J. Phys. (Moscow)* 9, 249 (1945).  
[2] N. Margolus and L. B. Levitin, The maximum speed of dynamical evolution, *Physica (Amsterdam)* 120D, 188 (1998).